

FINAL REPORT: MOLECULAR MECHANISMS OF HYPOPIGMENTATION IN CYSTINOSIS

I) Summary of the proposal

Patients with infantile cystinosis have hypopigmentation with, for Caucasian subjects, blond hair, blue eyes and a clear skin. However it seems that some patients, in particular African American patients, but also few Caucasian patients have no hypopigmentation. Unfortunately no correlation between cutaneous phenotype, severity of renal disease and genotype has been carried out. The causes of hypopigmentation have not been so far elucidated.

In humans, pigmentation results from the synthesis and distribution of melanin in skin, hair bulbs, and eyes. Melanin synthesis or melanogenesis is an enzymatic process, catalyzed by tyrosinase, tyrosinase-related protein 1 (Tyrp1) and dopa chrome tautomerase (DCT), which convert tyrosine to melanin pigments. This process takes place in melanocytes within lysosomes-related vesicles named melanosomes.

Two types of melanin are produced by melanocytes. Eumelanins are black/brown melanins with high photoprotective properties and pheomelanins are red/yellow sulfur containing pigments that provide no protection against the noxious effects of solar irradiation. Melanogenesis proceeds in three distinctive steps. The initial step is the production of cysteinyl-dopa, which requires dopa (the product of tyrosine hydroxylation by tyrosinase) and sulfur containing compounds such as cystine. The second step is the oxidation of cysteinyl-dopa to give pheomelanin, which continues as long as cysteinyl-dopa are present. The last step is the production of eumelanin, which begins only after most of the cysteinyl-dopa are depleted.

Further, melanin synthesis is also regulated by the pH of melanosomes: alkalization of melanosomes by an inhibitor of vacuolar ATPase increases melanin synthesis and stimulation of melanin synthesis by α MSH is accompanied by an increase in melanosome pH. These data indicate that melanin synthesis take place at neutral or alkaline pH. Since *CTNS* is a cystine/H⁺ co-transporter, alteration of *CTNS* function in cystinotic cells would also lead to an acidification of melanosomes and an inhibition of melanin synthesis.

Taking into account that **cystinosin transports cystine out of lysosome and that melanosomes are lysosome-related vesicles, it was tempting to propose that cystinosin was involved in the active melanosomal efflux of cystine and regulates thereby melanogenesis.** In cystinosis, cystinosin dysfunction might lead to an intramelanosomal cystine accumulation that could favor pheomelanin synthesis compared to eumelanogenesis or to a decreased intramelanosomal pH, which is an important parameter in melanin synthesis. Alternatively, accumulation of cystine in melanosome might be toxic for melanocyte leading to a decreased cell growth or an increased apoptosis sensitivity.

The aim of this project is to explain the molecular mechanisms of hypopigmentation in cystinosis. To reach this objective:

- A- we will determine the dermatologic phenotype of patients with infantile cystinosis to have an objective and quantitative evaluation of pigmentation disorders in this disease. This part of the project has started in March 2008.
- B- we will study the role of cystinosin in melanogenesis as well as in melanocyte growth and apoptosis

II) Cellular biology results.

A- *CTNS is a melanosomal protein*

First, real time PCR analysis of cystinosis gene (*Ctns*) expression in mouse adipocytes, liver, skeletal muscle, kidney and B16 mouse melanoma cells showed a strong expression of *Ctns* in mouse melanoma cells that was comparable at those found in kidney. Next, using a **CTNS-GFP** construct, we showed by immuno-fluorescence and biochemistry studies that CTNS-GFP co-localized with mature melanosomes (Fig. 1, A, B). Further, immune-precipitation of intact melanosome showed the presence of GFP-CTNS in TYRP1 containing vesicles (Fig 1, C). These data suggest that CTNS is a melanosomal protein.

B- *Regulation of Tyrosinase expression by CTNS*

We showed that *Ctns* silencing (siCTNS) inhibited cell pigmentation and reduced melanin synthesis by more than 50% compared to control cells (siCont) (Fig.2). This effect was due to a decrease in the tyrosinase level through a post-transcriptional process. Indeed, CTNS silencing induces a dramatic decrease in tyrosinase protein expression (Fig 3, A), but does not affect the expression of tyrosinase messengers (Fig.3, B). CTNS silencing does not affect *Tyrp1* and *DCT* expression. We hypothesized that CTNS might control tyrosinase stability/ degradation. Two pathways have been involved in tyrosinase degradation. One involves the proteasome and the other one involves cysteine proteases. Using the specific proteasome inhibitor MG132, we showed that proteasome inhibition did not prevent the decrease in tyrosinase expression evoked by CTNS specific siRNA. As positive control of MG132 functioning, we have shown an increase in HIF1 α expression in these conditions (not shown). On the other hand, the inhibition of cysteine protease, by E64 and leupeptin prevented the degradation of tyrosinase (Fig.4, lower panel). These data suggest that tyrosinase is degraded by lysosome proteases. However, E64 and leupeptin treatment does not allow the recovery of melanin synthesis in cells devoid of CTNS (Fig 4 Upper Panel).

C- *CTNS controls the pH of melanosome.*

Since CTNS is a cystine/H⁺ co-transporter, it was tempting to propose that *Ctns* silencing would affect melanosomal pH. Indeed, in cells transfected with si-*Ctns* we observed an increase in immunofluorescence labeling with Lyso-tracker® indicating that *Ctns* silencing led to an acidification of the intracellular vesicular compartments. To identify these intracellular vesicles we changed our technical approach. We used the *N*-(3-((2,4-dinitrophenyl)amino)propyl)-*N*-(3-aminopropyl)methylamine, dihydrochloride (DAMP), a weak base that accumulates in acidic compartments. DAMP was then localized by anti-DNP (dinitrophenol) antibodies. Melanosomes were identified by anti-Tyrp1 antibodies. In basal conditions, melanosomes (orange/red) appeared located around the nucleus and co-localized more or less with DAMP (green). After treatment with α MSH, melanosomes were found mainly at the cell periphery and little co-localization with DAMP could be observed, indicating that during cAMP induced differentiation melanosomes became less acidic. Interestingly, when cells were transfected with siCTNS, we observed a strong increase in the DAMP labeling (green) and most of the melanosomes appear yellow/green indicating that CTNS silencing caused an acidification of the melanosomes (Fig. 5.A). Interestingly treatment with bafilomycin a V-ATPase inhibitor restores both tyrosinase expression and melanin synthesis (Fig. 5. B).

D- Regulation of CTNS expression during melanocyte differentiation.

We have shown that forskolin increases *Ctns* mRNA in both normal human melanocytes and B16 melanoma cells (Fig 6, A) and activates the CTNS promoter (Fig 6, C). However, MITF, a transcription factor that mediates most of the effect of cAMP on melanocyte differentiation, is not involved in the regulation of CTNS by cAMP.

E- CTNS controls growth of melanoma.

We also investigated the effect of CTNS silencing on melanocyte growth. Using XTT method we observed a 50% decrease in cell growth after transfection with siCTNS (Fig.7.A). FACS analysis of DNA content showed that cells depleted in CTNS were blocked in G1 phase (Fig.7.B). No apoptosis (subG1) could be observed. Further western blot analysis with anti Phospho-pRB and anti-p27 antibodies showed that CTNS silencing decreases pRB phosphorylation and increased p27 expression (not shown), in total agreement with a G1 arrest. How CTNS can influence cell growth remain to be elucidated.

Note that CTNS silencing was verified in all the experiments by Q-PCR analysis. Si-CTNS induced 80 to 90% decrease in CTNS messengers.

F- Effect of CTNS knock-out on mice pigmentation

Ctns knockout mouse model was generated using a promoter trap approach by Cherqui et al. Mol. Biol. Cell. 2002. The truncated protein was mislocalized and nonfunctional. *Ctns*^{-/-} mice accumulated cystine in all organs tested, and cystine crystals, pathognomonic of cystinosis, were observed. *Ctns*^{-/-} mice developed ocular changes similar to those observed in affected individuals, bone defects and behavioral anomalies. Interestingly, *Ctns*^{-/-} mice did not develop signs of a proximal tubulopathy, or renal failure. We have shown in both C57bl6 and agouti mice with non functional *CTNS* a increased pheomelanin content in hair of this mouse compared to wild type mouse, suggesting that CTNS is able to favor eumelanogenesis probably by decreasing the intramelanosomal cystine concentration. Interestingly, these mice have the same coat color due to high basal level of eumelanin (Fig. 8). The absence of clinical phenotype in C57bl6 mice might a reminiscence of the picture observed in dark-skin patients who have no hypopigmentation.

G- Conclusions.

Taken together these data led us to propose the following hypothesis: Melanosomes derive from early endosomes. Four types of melanosomes can be identified by their morphology and their melanin content. It seems that type II melanosomes are more acidic than type III which contain tyrosinase and synthesize melanins. CTNS, which seems to be preferentially located within type III melanosomes, might participates in the alkalization of these melanosomes, favoring thereby melanin synthesis. In absence of CTNS, the pH of type III melanosomes remains acidic leading to the miss targeting of tyrosinase to lysosome and its subsequent degradation. Alternatively, the decrease in melanosome pH might led to the reactivation of lysosomal cysteine proteases such as cathepsins that work preferentially at acidic pH and that were found in melanososome. However, the lack of global

pigmentation defects in *CTNS* KO mice suggest the existence of additional regulatory mechanisms that remain to be elucidated.

III) Clinical evaluation

We have created a database of patients with infantile cystinosis in order to better define the clinical characteristics of the cutaneous involvement. For that, various parameters have been collected for each patient and his (her) parents, using a standardized questionnaire. A complete dermatological examination (including phototype) has been carried out among all patients and their parents to report other skin symptoms.

We have included 20 cystinosis patients. We have 21 relatives for 13 patients.

We have evaluated of the color of the skin (3 measures for each parameter) with a colorimeter in unexposed skin regions (inner part of the arms) and in exposed regions (forehead). This apparatus allows the measurement of the 3 cutaneous parameters (clearness, redness and the blue and yellow color of the skin) representative of skin color. All these data are currently under analysis.

- We have carried out a quantitative analysis of eumelanin and pheomelanin levels by HPLC and spectrophotometry in hair of 12 patients and their relatives. 9 of these patients have a significant decrease in eumelanin content compare to their relatives (Figure 9). 10 patients have a significant increase in pheomelanin content (Figure 10). These data clearly show that cystinosis patients have lighter and more pheomelaninic hair than their relatives.

- We have performed a non-invasive skin imaging with in vivo Confocal microscopy for 9 patients coupled to electron microscopy analysis for one patient. Nine patients (2 to 15 years) with cystinosis and nine controls were recruited for this study. Controls were patients without dermatologic or renal disease matched with age and phototype. Patients were 6 females and 3 males with a mean age of 11.8 years (range, 2.5 to 22). Nephropathic cystinosis was diagnosed based on a typical clinical presentation and a leukocyte cystine concentration > 3 nmol half-cystine per milligram of protein. All patients took systemic cysteamine (Cystagon, Orphan Europe, Paris, France) and cysteamine eye drops (cysteamine hydrochloride 0.1%, Pharmacie Centrale des Hôpitaux de Paris, Paris, France) since the diagnosis. Patients were examined at the Archet 2 Hospital in Nice (patients 1-3) or at Necker hospital in Paris (patients 4-9), France by the same examiner. The dermatologic evaluation included total body examination and evaluation of the phototype of patients, parents and when available siblings. Patient was considered to have a hypopigmentation when his phototype were lower than its family. A skin sample was obtained from patient 1 with his consent for electronic microscopy analysis.

A- Clinical features

Clinical and biological features of 9 patients are summarized in table I. In brief 6 patients reached an end stage renal disease and 4 of them were grafted. All patients excepted the youngest one have corneal crystal deposits at slit-lamp biomicroscopic analysis. Two patients (patient 1 and 8) have extra-renal involvement with hypothyroidism, and 3 patients have cutaneous hypopigmentation. Cysteamine therapy was initiated before one year old for all patients excepted for patient 2 and 8 because of delayed diagnosis (20 months and 10 years

old respectively). CTNS mutations and their functional repercussion were available for 7 patient..

B- ICM images

ICM images of forearm skin of all 9 cystinosis patients have been obtained in epidermis and upper dermis in all patients. Scattered bright particles at the level of the upper dermis were observed throughout all examined skin. The brightness intensity of particles was variable for a given patient and between patients. The diameters were from 1 μm to up to about 10 μm and appeared as round bodies. Some lanceolate particles were seen. The amount of particles were different i.e. 6 of 9 patients showed numerous (+++) particles, one patient showed some (++) , one patient showed a few (+) particles and one patient very few (+/-) particles (Figure 11). The repartition of particles in dermis was diffuse but heterogeneous, with an accumulation around or in the vessels. The intra or extra cellular position of crystals was impossible to discriminate. Because of thickness of the skin, the lower dermis was not valuable.

Patient 6 and 7 had a *in vivo* confocal microscopy of cornea with the following results: patient 6 score in the right eye of 6,75/28. C, D, patient 7 score in the right eye of 3,35/28 (Figure 12). The exam of forearm skin of all 9 controls showed no particles at the level of the dermis throughout all skin.

C- EM images

EM showed intracytoplasmic crystal deposits in fibroblasts (Figure 13). No extracellular deposits were seen. Epidermis was structurally normal. No anomalies of keratinocytes, melanocytes, masts cells, endocytes or nerves were observed.

D- Correlations

We analyzed whether the amount of particles is related to clinical severity, age of patients or CTNS mutation. There was no clear relation between phototype, severity of the renal disease, duration of cysteamine therapy, hemi-cystine leukocyte level, CTNS mutation and the number of particles in the dermis. All patients older than 13 years have high level of crystal deposits in skin and skin infiltration suggesting an accumulative process. However one 4-year-old patient also has a high level of crystal deposits without skin infiltration. There was a good correlation between corneal and dermis amount of crystal deposits seen in *in vivo* confocal microscopy for the two patients where data were available. Finally, all patients with extra renal involvement have high level of cystine in the dermis.

E- Conclusions

In this study we have shown, using for the first time the *in vivo* confocal microscopy on skin of young cystinosis patients that all patients have cystine deposits in skin visualized as round or oval shape dermal particles of variable size. These particles are specific of the disease since no particle has been seen in control skin. Moreover, we showed by histological analysis, crystalline intracytoplasmic cystine deposits in fibroblasts in reticular dermis confirming our data. Particles distribution was heterogeneous with a clear perivascular accumulation. The exam was quick (five minutes), painless and well tolerated by all patients, even the younger ones.

Comparison of patient's RCM images allows us to develop a first semi-quantitative evaluation of crystal deposits in dermis. Interestingly, our results were similar to those obtained by *in vivo* confocal microscopy of the eye for two patients with the same amount of particles in skin and cornea but a different distribution, suggesting a different accumulative mechanism.

There was no correlation between the severity of renal involvement, the presence of hypopigmentation and the level of crystal deposit in skin. The early outcome of such anomalies suggests more a specific cellular dysfunction of cystinosin in renal proximal tubular cells and melanocytes than an accumulative process. Consistent with this hypothesis, mice KO for *Ctns*, do not develop tubulopathy or hypopigmentation despite of renal and skin cystine accumulation. Beside these precocious manifestations, a wide range of later involvement has been described like photophobia, hypothyroidism, central or peripheral neuropathy, myopathy, diabetes mellitus and skin infiltration. These late manifestations are thought to be secondary to cystine accumulation in tissues and their progressive destruction. As expected, all patients with extra renal manifestations have high level of crystal deposit in dermis and no patient with low level of crystal deposits have extra renal involvement. The amount of crystal deposits seems to increase with the age of patients but was not well correlated. Interestingly, some patients with high level of dermis crystal deposits have no detectable extra renal symptoma. Moreover one of these patients has no skin infiltration. These data suggest that skin infiltration is not secondary to cystine accumulation in dermis but rather to a fibroblast dysfunction with abnormal collagen and or elastic fiber synthesis and that crystal deposit in skin could be a predictive marker of extra-renal involvement.

If cysteamine therapy has considerably delayed the onset of clinical manifestations, it does not cure patients. Moreover some patients despite a good treatment intake and normalized leukocyte cystine level have an unexplained and unpredictable severe renal and/or extra-renal course. Clinical quantification of the amount of cystine crystal deposit in dermis by confocal microscopy *in vivo* could be a good and independent prognosis criterion of extra renal progression of infantile cystinosis.

IV) Figure legends.

Figure 1: Subcellular localization of Ctns. (A) Immunofluorescence of B16 melanoma cells, treated for 24hours with forskolin, transfected with *CTNS*-GFP (green) and labeled with an anti-tyrp1 or anti-pmel17 antibody (red). Co-localization of CTNS-GFP with Tyrp1 or Pmel17 (yellow). (B) Same experiment at higher magnification shows colocalization (yellow) of CTNS-GFP (green) and Tyrp1 (red). (C) Immunoprecipitation of intact melanosomes using an anti-GFP antibody in B16 melanoma cells transfected with *CTNS*-GFP or GFP alone. Western blot of total (tot), and immunoprecipitated (IP) proteins using anti GFP, Rab4 and tyrosinase antibodies.

Figure 2: Effects of Ctns silencing on B16 melanoma cells pigmentation. (A) pellets of cells treated (FSK) or not for 48 hours by forskolin (20 μ M) and transfected by si-*Ctns* or control siRNA (si-Sc). (B) Direct light and phase contrast microscopy visualization of cells treated by FSK for 48h and transfected by si-*Ctns* or si-Sc. (C) Spectrophotometric measurement of melanin content in cells transfected by si-*Ctns* or si-Sc and treated or not by FSK.

Figure 3: Effects of Ctns silencing on enzymes of melanogenesis. (A) western blot analysis on B16 cells melanoma cells transfected by si-*Ctns* or si-Sc and stimulated by FSK for 48

hours. (B) Q-PCR analysis of *Ctns* and *tyrosinase* mRNA levels in B16 cells melanoma cells transfected by si-*Ctns* or control si-Sc and stimulated or not by FSK for 48 hours.

Figure 4: Effects of cysteine protease inhibitors on tyrosinase expression. (A) western blot analysis of B16 cells melanoma cells transfected with si-*Ctns* or si-Sc, stimulated or not by FSK for 48 hours. This experiment was carried out in absence of protease inhibitor (Cont) or in presence of 15 μ M E64 and 10 μ M leupeptin (E64+LEU). Upper panel, B16 cell pellets are shown. Lower panel, tyrosinase expression was analyzed by western blot with anti-tyrosinase antibody (PEP7, 1/250).

Figure 5: Effects of *Ctns* silencing on melanosomal pH. (A) B16 melanoma cells were transfected with si-*Ctns* or si-Sc, treated (MSH) or not by α MSH, 0.1 μ M, for 48h and then incubated for 15 min with DAMP 100 μ M. Cells were fixed, permeabilized and labeled with anti-DNP (green) and anti-Tyrp1 (red) antibodies. (B) Western blot analysis of B16 cells melanoma cells transfected with si-*Ctns* or si-Sc, stimulated or not by FSK for 48 hours. This experiment was carried out in absence (Cont) or in presence of 5mM bafilomycin (Bafilo). Upper panel, B16 cell pellets are shown. Lower panel, tyrosinase expression was analyzed by western blot with anti-tyrosinase antibody (PEP7, 1/250).

Figure 6: Regulation of CTNS expression during melanocyte differentiation. (A) RNA levels of *Ctns* in MHN treated (FSK) or not (0) by forskolin (20 μ M) for 48hours, (B) Alignment of human and mouse of the *ctns* promoter performed using BLAST program (NCBI). Exon 1 of the human and murine *ctns* gene is shown by black arrow. E boxes are indicated in red (C) B16 cells were transfected in lipofectamine with 0.3 μ g of *pctns*-wt, 0.05 μ g of pCMVGAL and 0.2 μ g of pMITF or not. After 24 h with forskolin, luciferase activity was normalized by the β -galactosidase activity and the results were expressed as fold stimulation of the basal luciferase activity from un-stimulated cells. Data are means \pm SE of five experiments performed in triplicate.

Figure 7. Effects of *Ctns* silencing on melanocyte growth. (A). B16 melanoma cells were transfected with si-*Ctns* or si-Sc and cell viability was assessed using the cell proliferation kit II (XTT; Roche Molecular Biochemicals) according to the manufacturer's protocol. (B). *Flow cytometry analysis.* B16 melanoma cells were transfected with si-*Ctns* or si-Sc, detached in PBS/EDTA 1 mM and centrifugated for 5 minutes at 2000G at RT. Pellets were resuspended in 200 μ L of citrate buffer pH 7.6 (sucrose 250mM, Tris-sodium citrate 40mM) and stained with propidium iodine at 4°C for 1 hour. Fluorescence was measured by using the FL2 channel. (C) Quantification of FACS analysis.

Figure 8. Effect of CTNS knock-out on mice pigmentation. Upper panels show a picture of wild type and CTNS^{-/-} mice in C57bl6 and Agouti background. Lower panels show the quantification by HLPC of Eumelanin and Pheomelanin content in mouse hairs.

Figure 9. Clinical evaluation of hair pigmentation in cystinosis patients: eumelanin content.

Hair samples were cut to about 5 mm length with scissors, and their weights were accurately measured. About 1-2 mg of hair was subjected to alkaline hydrogen peroxide oxidation. PTCA, a specific eumelanin marker, was analyzed by HPLC-UV detection and eumelanin content was calculated as previously described.

Figure 10. Clinical evaluation of hair pigmentation in cystinosis patients: pheomelanin content.

Hair samples were cut to about 5 mm length with scissors, and their weights were accurately measured. About 1-2 mg of hair was subjected to reductive hydrolysis with hydroiodic acid. 4-AHP, a specific pheomelanin marker, was analyzed by HPLC-EC detection. Pheomelanin (PM) content was calculated as previously described.

Figure 11: *In vivo* confocal images of the skin. *In vivo* confocal microscopy images (4 mm x 4mm) of cystinosis patients skin (A, B, C) and control skin (D). Bright particles were seen around or in the vessels (arrows) at the level of dermis in cystinosis patients and were absent in control skin.

Figure 12: *In vivo* confocal images of the cornea. *In vivo* confocal microscopy images (400 ×400 μm) of the cornea of patients with nephropathic cystinosis showing crystals within the anterior corneal stroma. A, patient 6 with a score in the right eye of 6,75/28. C, patient 7 with a score in the right eye of 3,35/28. B and D show the corresponding *In vivo* confocal images of the skin.

Figure 13: Intracytoplasmic crystal deposits in dermis fibroblasts. Electron microscopy analysis of the dermis of skin from cystinosis patient 1. Numerous parallelogram structures can be observed within fibroblasts, corresponding to the shadow of cystine crystals.

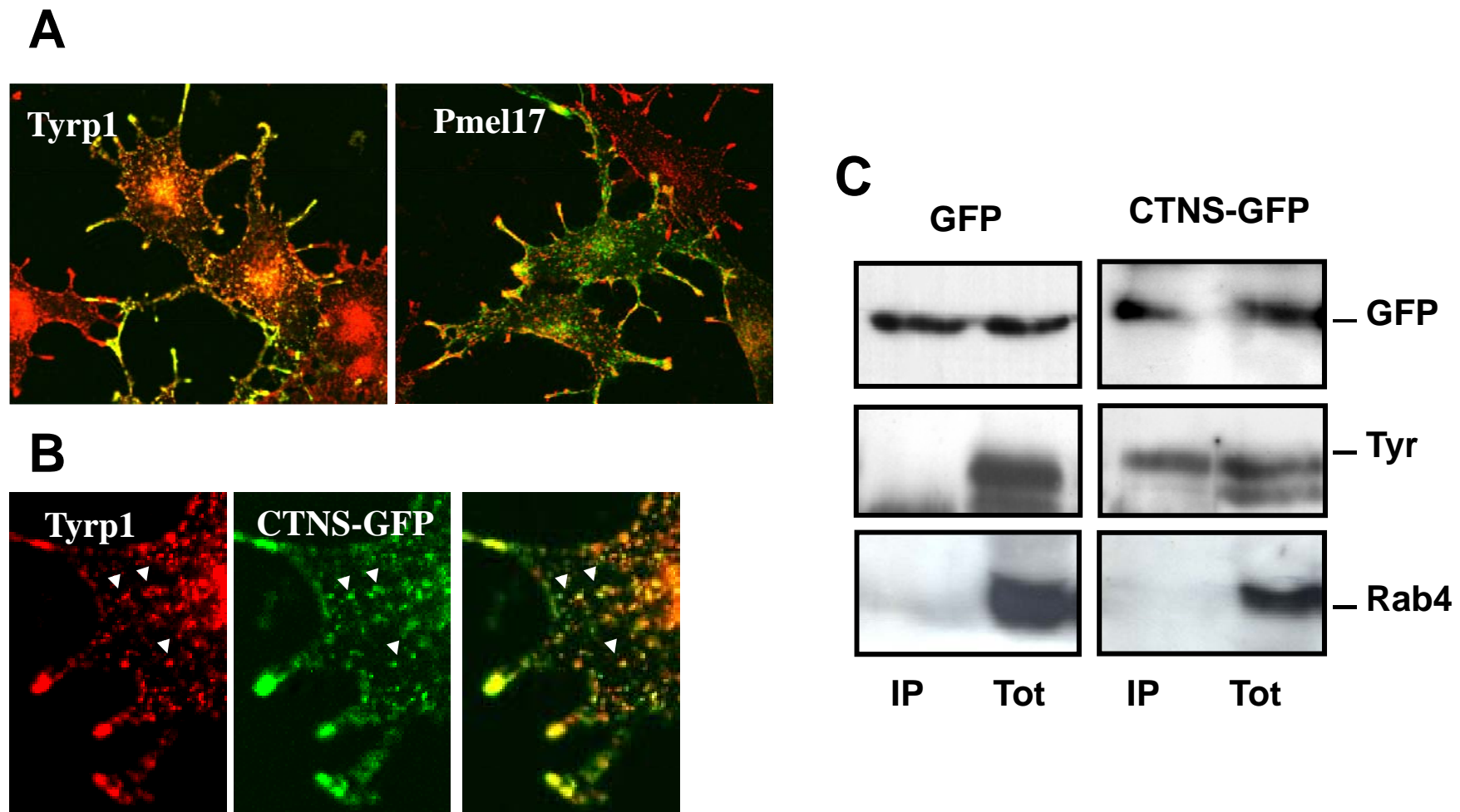


FIG.1

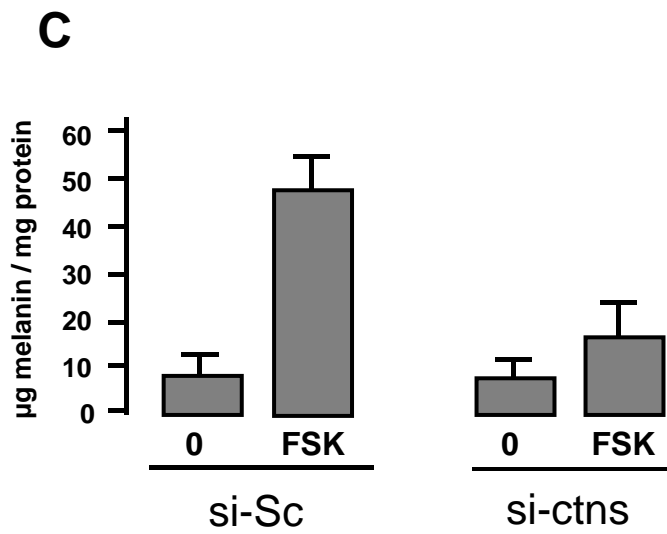
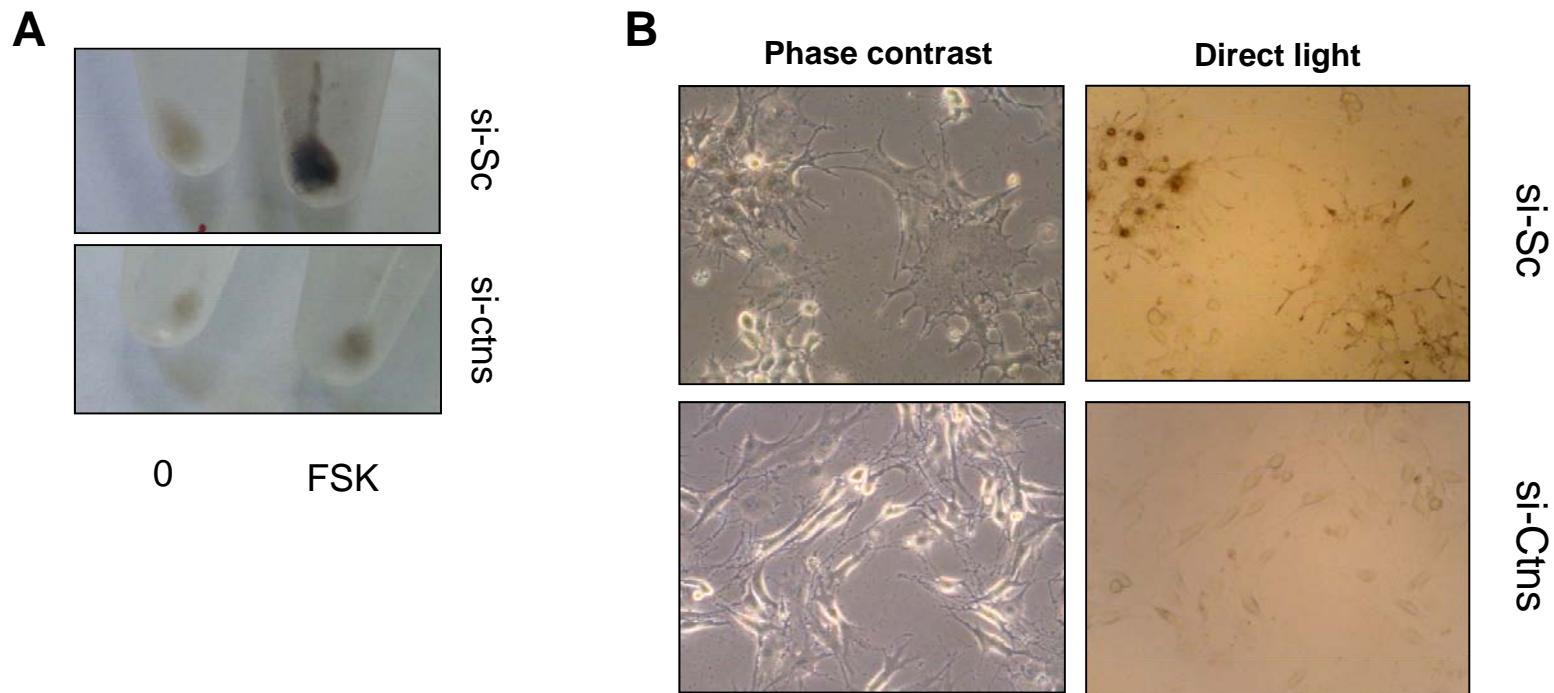


FIG.2

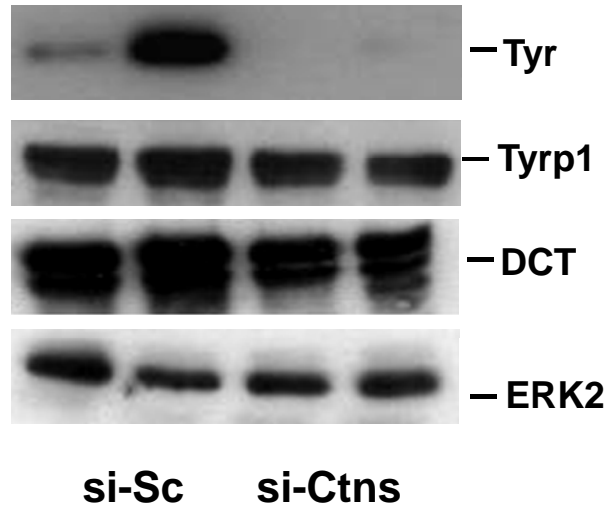
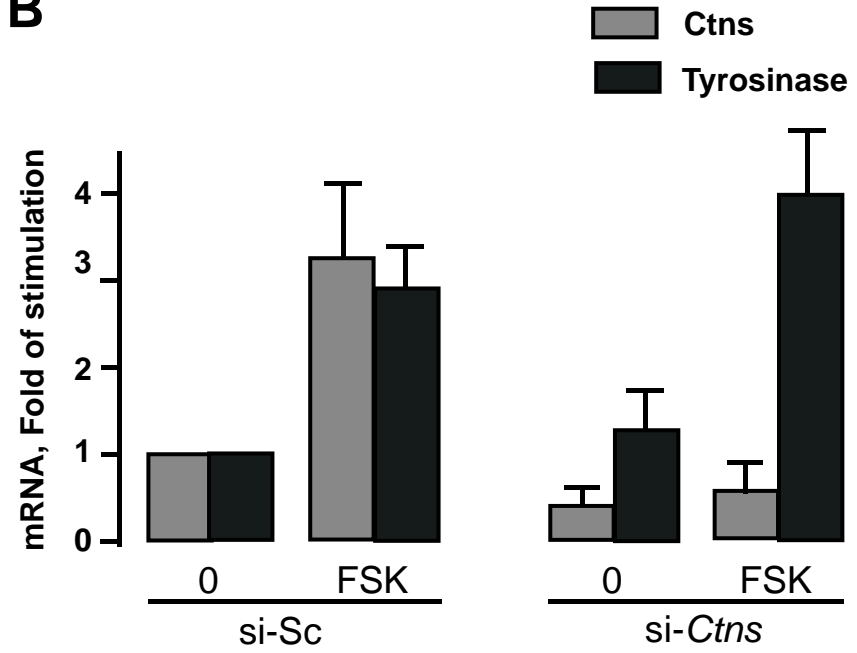
A**B**

FIG.3

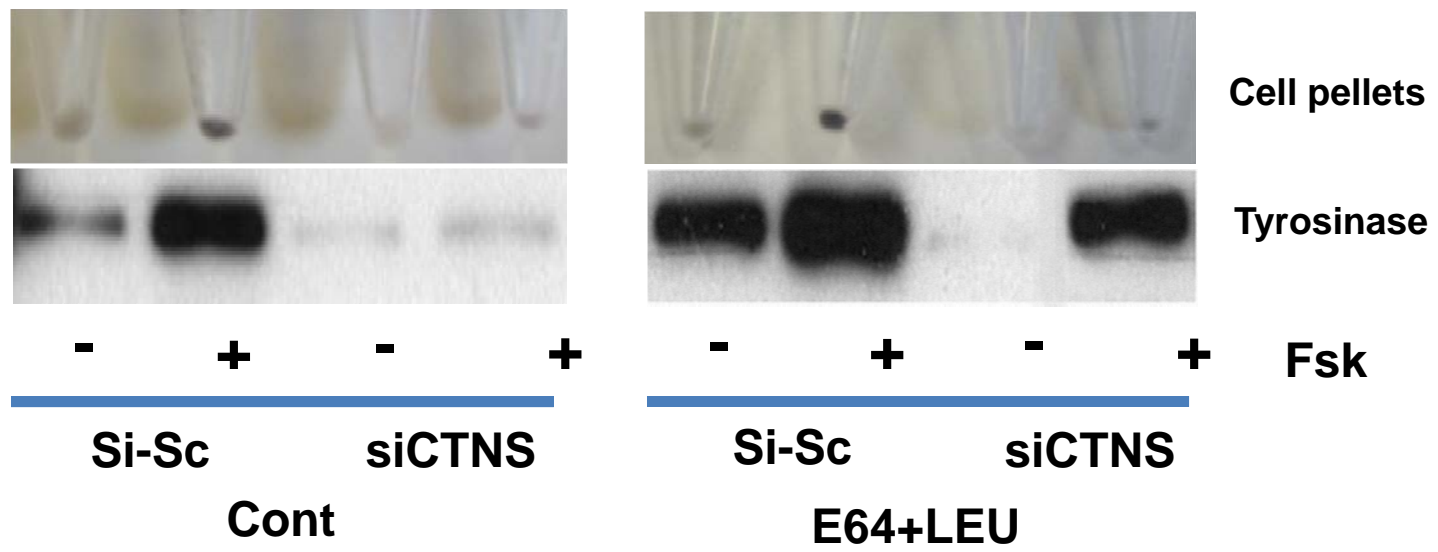


FIG.4

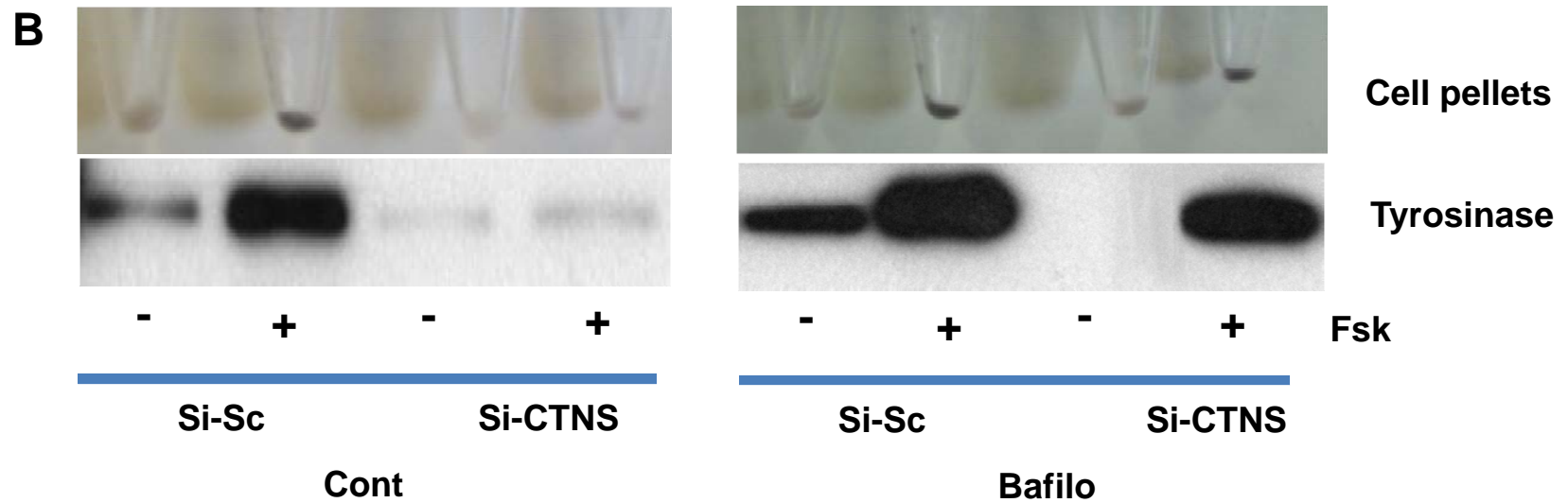
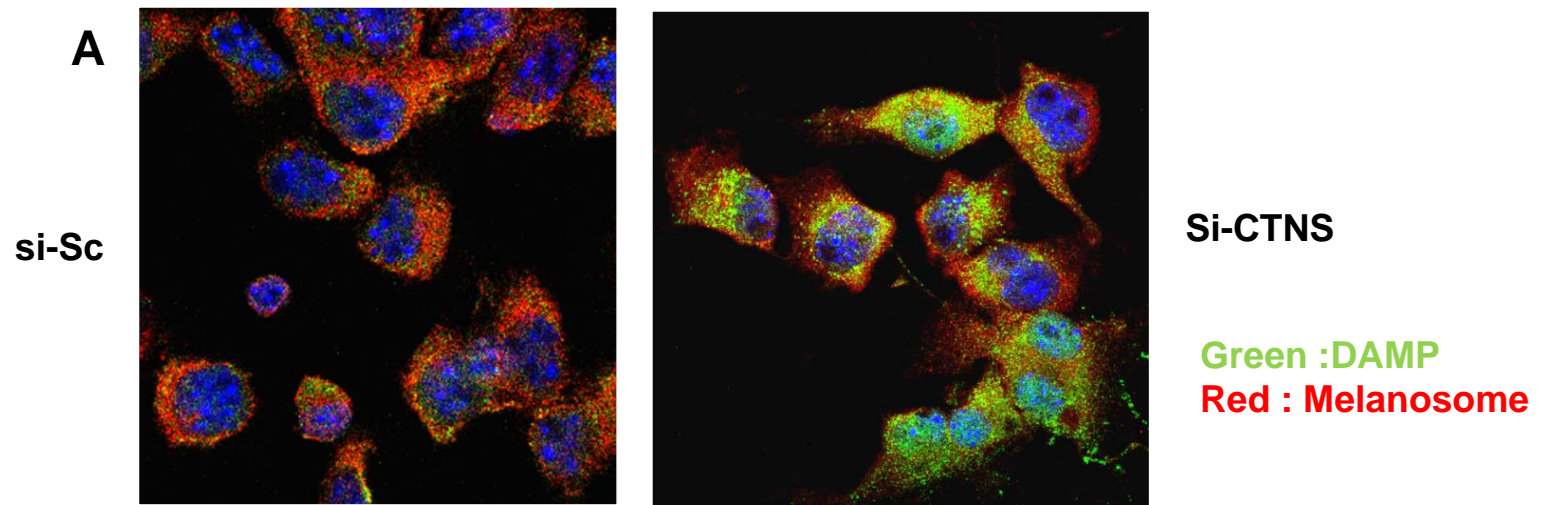


FIG.5

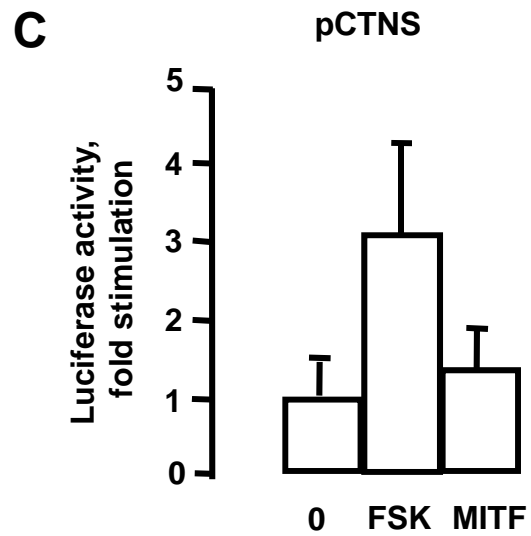
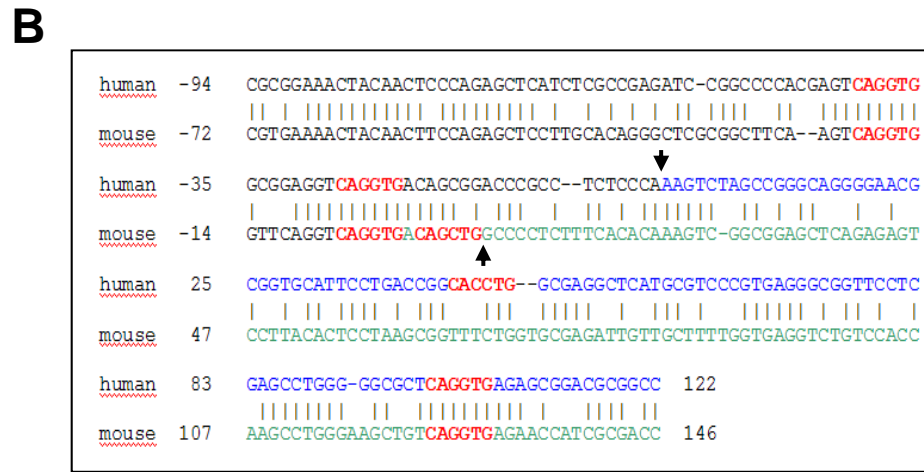
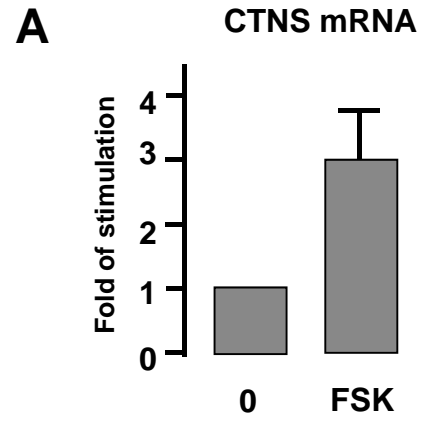


FIG. 6

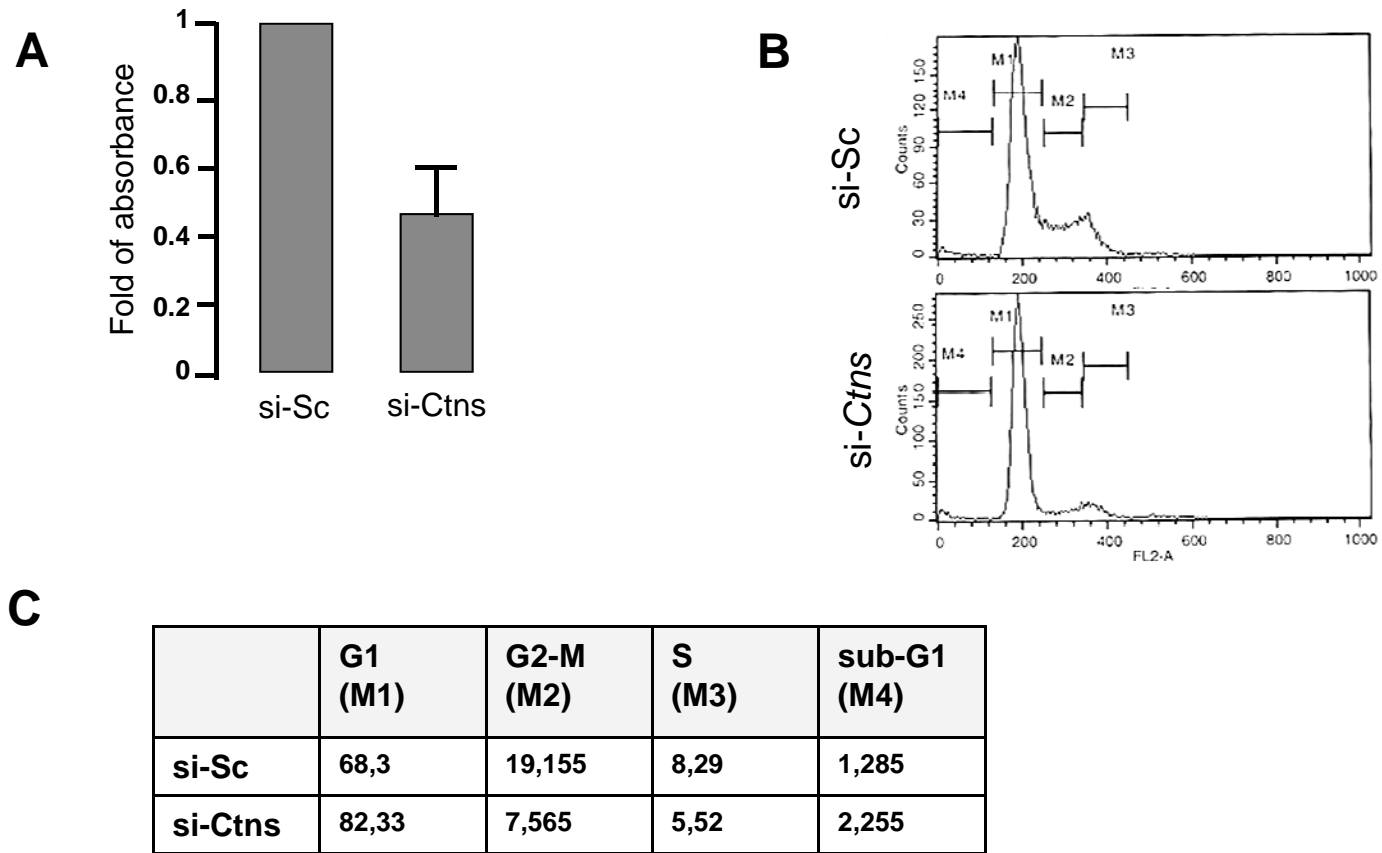
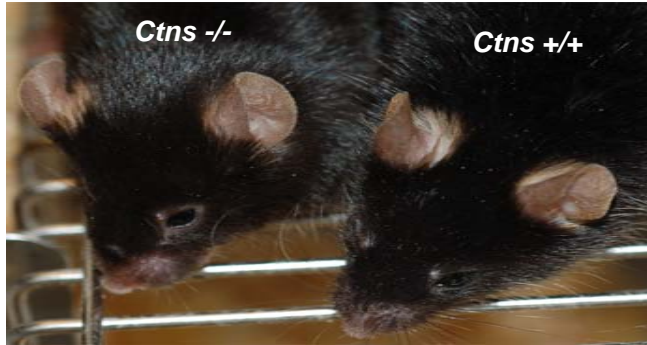


FIG. 7

C57bl6



Agouti

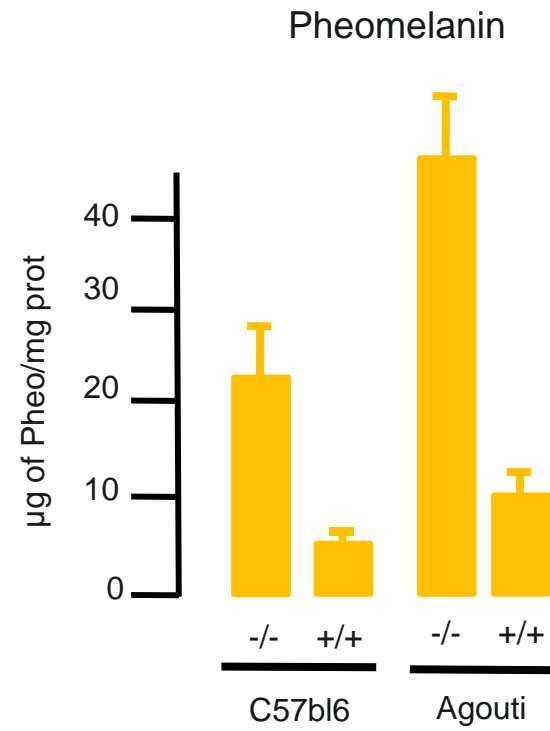
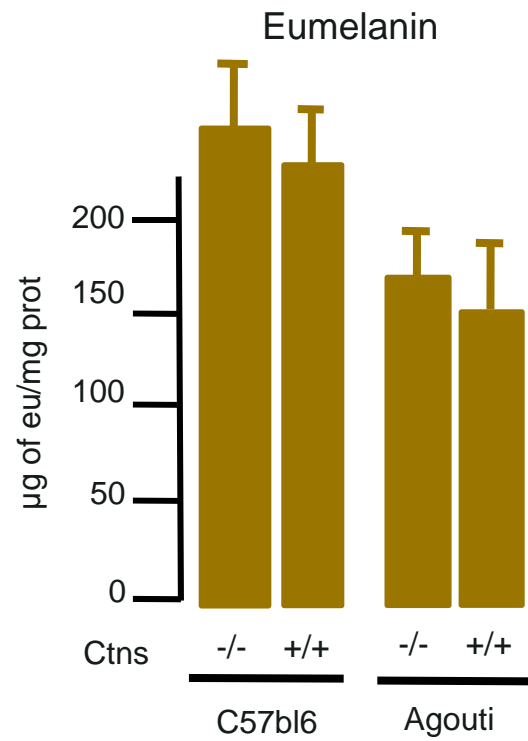


FIG.8

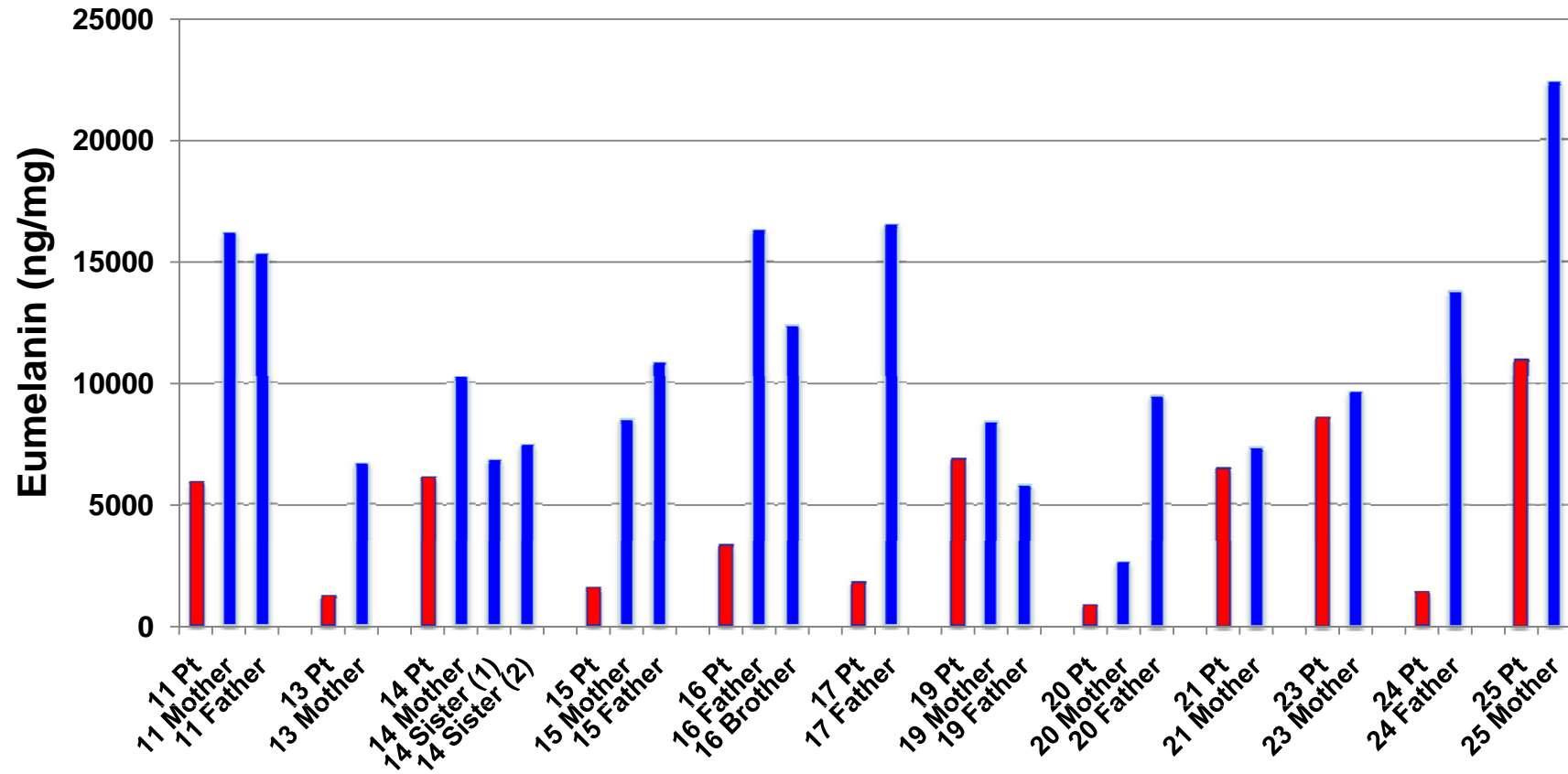


FIG.9

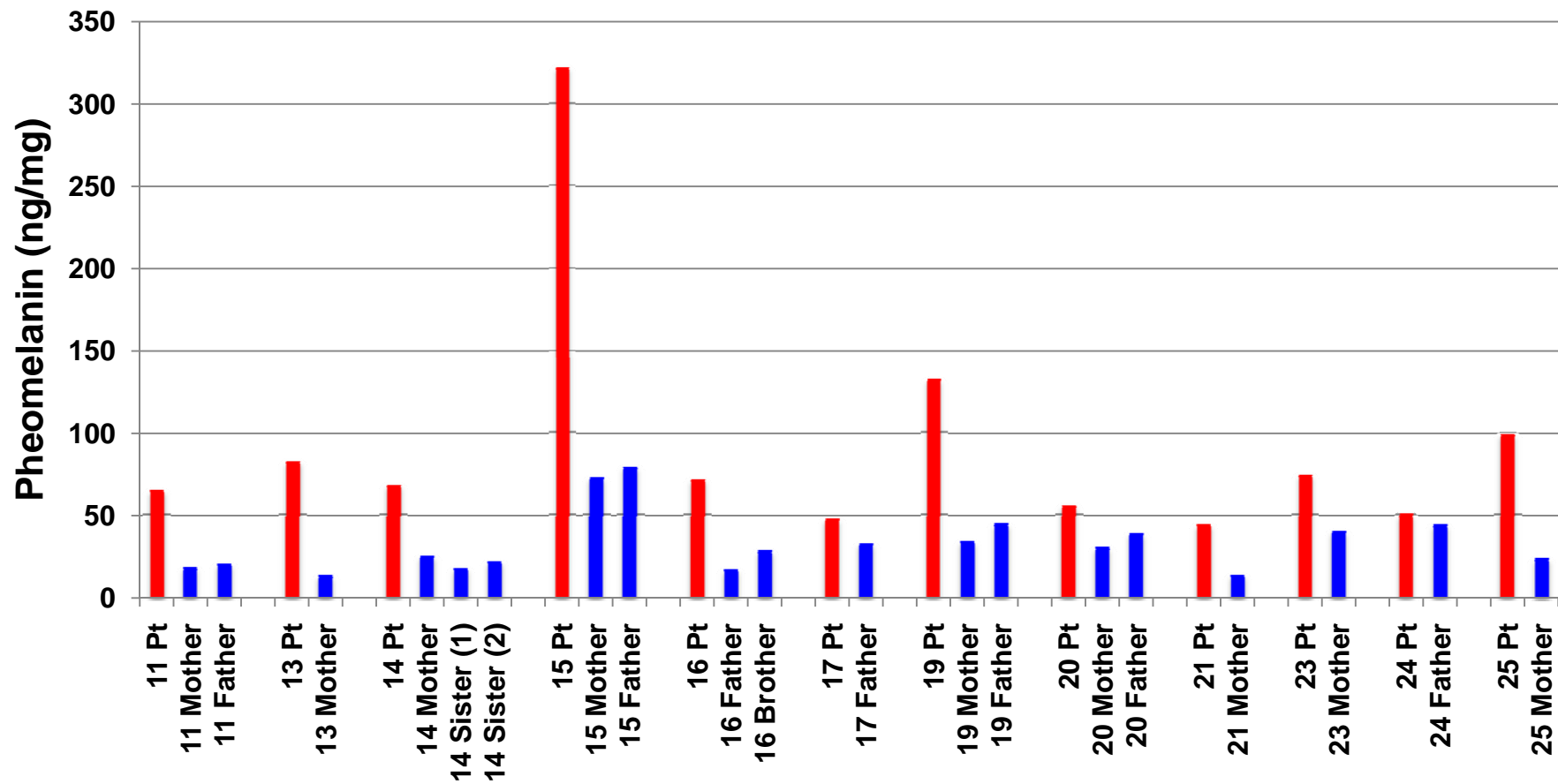


FIG.10

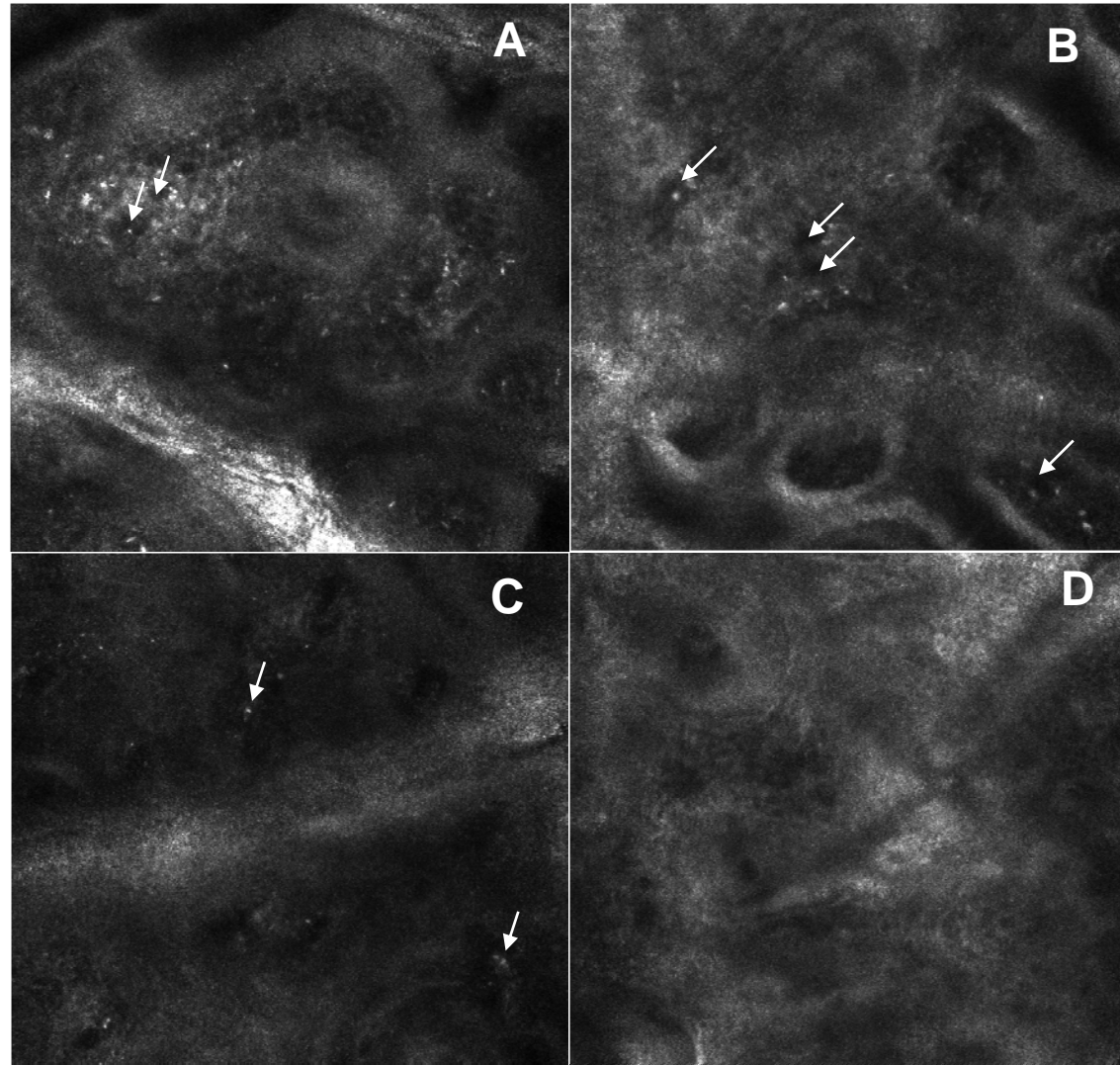


FIG. 11

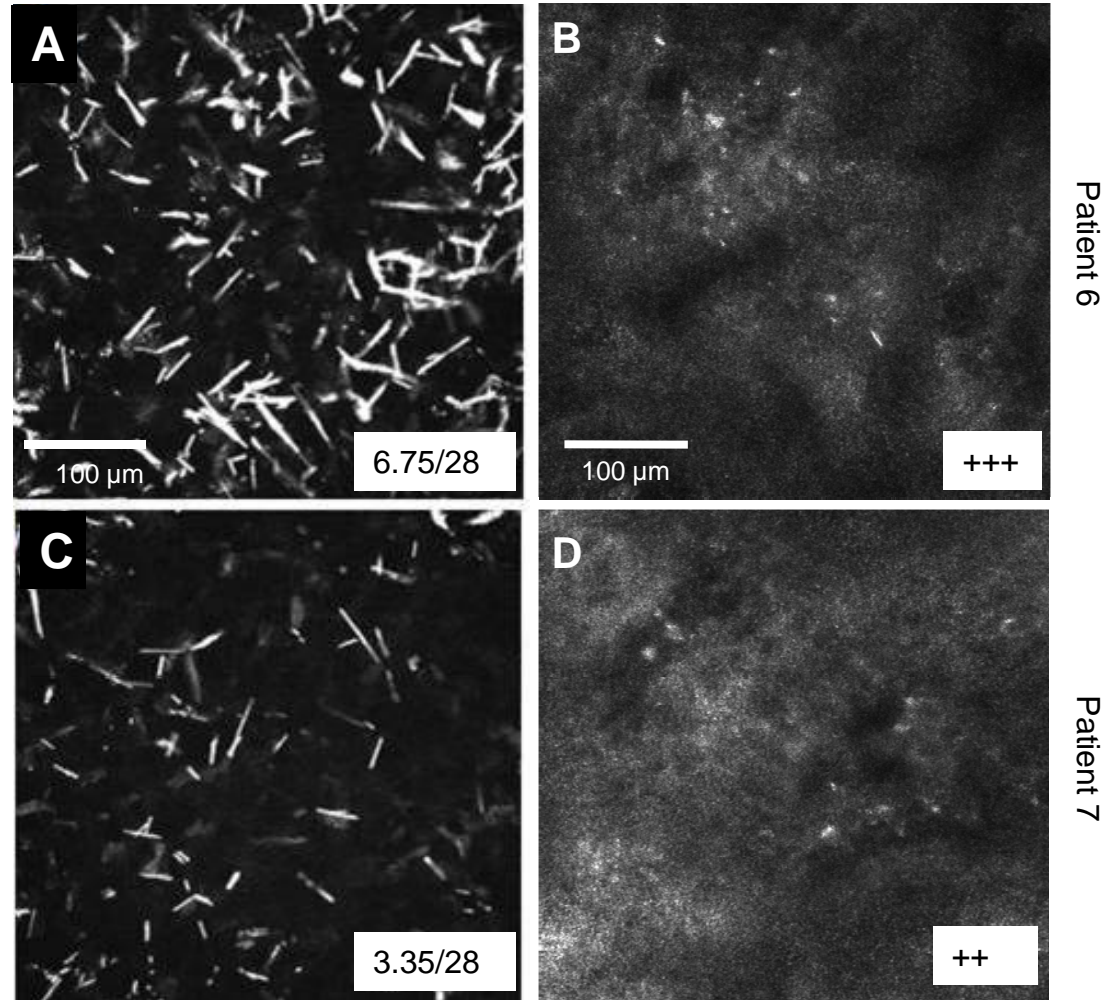


FIG. 12

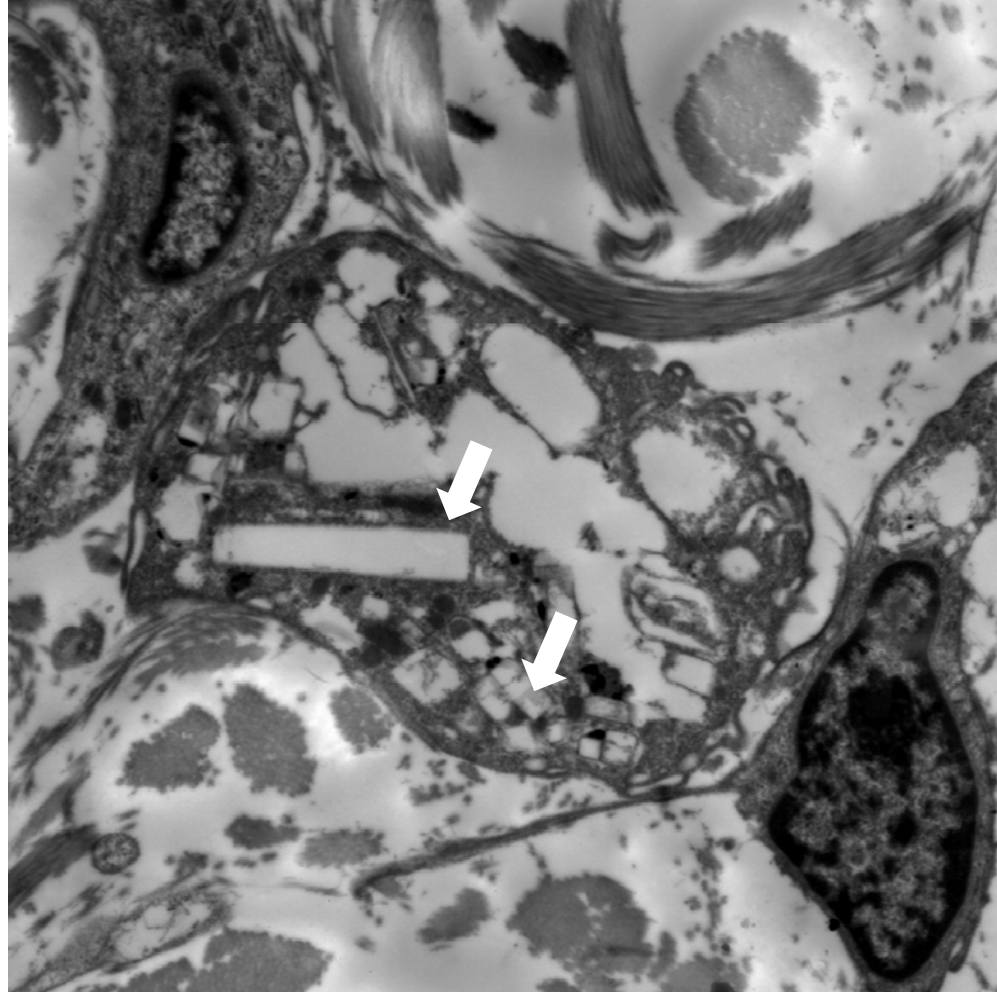


FIG. 13